Changes in global-mean precipitation in response to warming, greenhouse gas forcing and black carbon

K. Frieler,[1] M. Meinshausen,[1] T. Schneider von Deimling,[1] T. Andrews,[2] and P. Forster[2]

Received 1 November 2010; revised 17 December 2010; accepted 30 December 2010; published 16 February 2011.

[1] Precipitation changes are a key driver of climate change impacts. On average, global precipitation is expected to increase with warming. However, model projections show that precipitation does not scale linearly with surface air temperature. Instead, global hydrological sensitivity, the relative change of global-mean precipitation per degree of global warming, seems to vary across different scenarios and even with time. Based on output from 20 coupled Atmosphere-Ocean-General-Circulation-Models for up to 7 different scenarios, we discuss to what extent these variations can be explained by changes in the tropospheric energy budget. Our analysis supports earlier findings that long- and shortwave absorbers initially decrease global-mean precipitation. Including these absorbers into a multivariate scaling approach allows to closely reproduce the simulated global-mean precipitation changes. We find a sensitivity of global-mean precipitation to tropospheric greenhouse gas forcing of $-0.42 \pm 0.23\%/(W/m^2)$ (uncertainty given as one std of inter-model variability) and to black carbon emissions of $-0.07 \pm 0.02\%/(Mt/yr)$. In combination with these two predictors the dominant longer-term effect of surface air temperatures on precipitation is estimated to be $2.2 \pm 0.52\%/K$ – much lower than the 6.5%/K that may be expected from the Clausius-Clapeyron relationship. **Citation:** Frieler, K., M. Meinshausen, T. Schneider von Deimling, T. Andrews, and P. Forster (2011), Changes in global-mean precipitation in response to warming, greenhouse gas forcing and black carbon, *Geophys. Res. Lett.*, *38*, L04702, doi:10.1029/2010GL045953.

1. Introduction

[2] Relative humidity is observed to stay approximately constant under global warming [*Trenberth et al.*, 2007]. Therefore, if precipitation was driven by the availability of moisture, one would expect an increase of about 6.5%/K from the Clausius Clapeyron relationship between temperature change and saturation vapor pressure [*Mitchell et al.*, 1987; *Allen and Ingram*, 2002]. 20-yr long satellite observations seem to support such an increase [*Wentz et al.*, 2007], although observed precipitation trends strongly differ across data sources [*Trenberth et al.*, 2007; *Arkin et al.*, 2010]. On a longer timescale, current Atmosphere-Ocean-General-Circulation-Models (AOGCMs) show a much weaker global hydrological sensitivity (HS) of about 1–3%/K (median = 1.7%/K after *Held and Soden* [2006] and 1.4%/K after *Liepert and Previdi* [2009]). The tropospheric energy budget seems to set a more severe constraint on simulated precipitation changes than availability of moisture [e.g., *Mitchell et al.*, 1987; *Allen and Ingram*, 2002; *Held and Soden*, 2006; *Liepert and Previdi*, 2009].

[3] Changes in forcing agents might change global-mean precipitation in two ways: (1) via changes in global-mean surface air temperature and associated climate feedbacks, on a "slow" timescale of years or (2) by changes to the tropospheric energy budget due to the presence of the forcing agent itself, on a "fast" timescale of days or weeks.

[4] The response to global-mean surface air temperature, ΔT, has been shown to be well described by $\alpha\Delta T$, [e.g., *Lambert and Webb*, 2008; *Andrews et al.*, 2009; *Ming et al.*, 2010] with α being approximately independent of the forcing agent [*Andrews et al.*, 2010]. *Previdi* [2010] analysed AR4 AOGCMs simulations to split up the feedback term into a temperature, water vapor, and cloud related component. A "fast" response to the change in tropospheric heating occurs as soon as purely radiative top of the atmosphere (TOA) and surface forcing differ. Higher TOA than surface forcing induces a tropospheric heating that decreases the vertical temperature gradient (lapse rate) - thereby stabilizing the atmosphere, damping convection and precipitation [*Lambert and Allen*, 2009; *Dong et al.*, 2009]. Given the small heat capacity of the troposphere and assuming small changes in tropospheric temperatures, conservation of its energy budget dictates that any tropospheric radiative forcing has to be balanced by sensible or latent heat fluxes – with the latter shown to be dominant, mainly on the basis of instantaneous CO_2 doubling experiments [e.g., *Mitchell et al.*, 1987; *Allen and Ingram*, 2002; *Yang et al.*, 2003; *Lambert and Faull*, 2007; *Andrews et al.*, 2009]. Other GHGs are expected to have a qualitatively similar effect as CO_2 on the tropospheric energy budget and hence on precipitation. Recently, black carbon (BC) aerosols gained more attention in the context of global HS [*Lambert and Allen*, 2009; *Andrews et al.*, 2010; *Ming et al.*, 2010; *Previdi*, 2010]. Absorbing shortwave radiation BC shows a positive TOA forcing (therefore increasing global-mean temperature, and so precipitation) while radiative surface forcing is estimated to be negative [*Ramanathan et al.*, 2001]. In addition to decreasing sensible heat fluxes at lower layers, the change in atmospheric radiative cooling also induces strong near-instantaneous reductions in latent heating [*Andrews et al.*, 2010; *Lambert and Allen*, 2009], which can even cancel the increase in precipitation expected from the associated surface warming [*Ming et al.*, 2010].

[5] For scattering aerosols (e.g., tropospheric sulfate aerosols or stratospheric volcanic aerosols) and changes in solar irradiance, TOA forcings are very similar to surface radiative forcings. Not considering possible interactions

[1]Earth System Analysis, Potsdam Institute for Climate Impact Research, Potsdam, Germany.
[2]School of Earth and Environment, University of Leeds, Leeds, UK.

0094-8276/11/2010GL045953

with BC, their "fast" effects on global precipitation are shown to be small [*Lambert and Faull*, 2007; *Andrews et al.*, 2010], although they might play an important role for regional precipitation [*Ramanathan et al.*, 2001].

[6] Usually, individual climate models were used to analyze the effects of different forcing agents separately. To our knowledge there is only one approach to extract the individual contributions from nine transient multi-forcing 20th century AOGCM runs [*Lambert and Allen*, 2009]. We build on this approach, test various predictors and quantify the unexplained inter-scenario variability of global HS.

2. Tropospheric Energy Budget

[7] The energy balance equation for the troposphere can be written as:

$$L\Delta P + \Delta SH = \alpha\Delta T + \Delta R \quad (1)$$

with specific latent heat L, $L\Delta P$ being the change in latent heat release due to changes in precipitation ΔP, ΔSH the change in sensible heat flux, $\alpha\Delta T$ the net change of radiative fluxes in and out of the troposphere due to changes in global-mean surface air temperature and associated climate feedbacks, and ΔR being the near-instantaneous tropospheric forcing. We split ΔR according to the forcing agents expected to be most relevant for precipitation changes, namely GHGs and BC. We furthermore assume that ΔSH can be split into additive components ($\Delta SH = \Delta SH_T + \Delta SH_{GHG} + \Delta SH_{BC}$) and that each of them can be related to the latent heat flux contribution by agent- or temperature specific Bowen Ratios ($B_X = \Delta SH_X/(L\Delta P_X)$, with X being T, GHG or BC). Thus, for relative precipitation change $\Delta P/P$ equation (1) can be rewritten as:

$$\Delta P/P = k_T * \Delta T + k_{GHG} * \Delta R_{GHG} + k'_{BC} * \Delta R_{BC}, \quad (2)$$

where $k_T = \alpha/(LP(1 + B_T))$, $k_{GHG} = 1/(LP(1 + B_{GHG}))$, and $k'_{BC} = 1/(LP(1 + B_{BC}))$.

3. Data and the Statistical Model

[8] To test whether equation (2) is able to explain variations in simulated global HS we apply a multivariate regression to data from 20 AR4 AOGCMs as available from the CMIP3 model archive (http://www-pcmdi.llnl.gov/ipcc/about/ipcc.php).

[9] We use the complete set of past (20c3m), future (commit, sresb1, sresa1b, sresa2), and idealized CO_2-only scenarios (1pctto2x, 1pctto4x), if available, including up to 5 ensemble runs for each of the seven scenarios. For each simulation we calculate decadal averages $(\Delta P/P)_{i,j}$ of global-mean precipitation changes (relative to the linear trend of the control run data) with i indicating the model and j the scenario. To explain $(\Delta P/P)_{i,j}$, we include the following three predictors, henceforth called "basic" predictors:

[10] 1. ΔT: decadal average of global-mean temperature change with respect to the linear trend of the control run.

[11] 2. ΔR_{GHG}: weighted sum of adjusted TOA forcings (F^{TOA}) with respect to the control runs based on the assumption that the tropospheric forcing of each GHG component is proportional to its adjusted TOA forcing. *Andrews et al.* [2010] found the same ratio of surface to TOA forcings for two different levels of CO_2 concentrations supporting the proportionality assumption at least for CO_2. Agent-specific weightings account for the fact that the ratio of ΔR_{GHG} to F^{TOA} may differ from forcing agent to forcing agent (see Figure S1 of the auxiliary material).[1] Assuming the ratio of agent specific weights to be model independent represents an additional limitation discussed in section 5. Adjusted TOA forcings are taken from AOGCM-specific emulations [*Meinshausen et al.*, 2008].

[12] 3. E_{BC}: global BC emissions, as provided by the AOGCM groups (see Figure S2). Given the relatively short atmospheric residence time of BC, E_{BC} is assumed to be proportional to tropospheric BC forcing ($\Delta R_{BC} \sim \beta E_{BC}$). High correlations between GHG and BC forcings in the 20c3m run that hindered *Lambert and Allen* [2009] analysing BC as separate regressor are less a problem in this study because we analyse both idealized and several multi-forcing scenarios. Given the above approximations, our model is described by:

$$\begin{aligned}(\Delta P/P)_{ij} = &\left(k_T + r_T^{mod,i} + r_T^{scen,i,j}\right)\Delta T \\ &+ \left(k_{GHG} + r_{GHG}^{mod,i}\right) * \Delta R_{GHG} \\ &+ \left(k_{BC} + r_{BC}^{mod,i}\right) * E_{BC} + \varepsilon_{ij}\end{aligned} \quad (3)$$

with k_T, k_{GHG}, and $k_{BC} = \beta\, k'_{BC}$ being the central (multi-AOGCM mean) estimates of the scaling coefficients that are equal or proportional to the coefficients introduced in equation (2). ε describes the residual variability of $\Delta P/P$ not explained by the predictors. The "random effects" framework [*Pinheiro and Bates*, 2000] applied here explicitly allows for AOGCM specific deviations ($r_X^{mod,i}$) from the central scaling coefficients, assumed to stem from normal distributions around zero. We optionally allow for normally distributed scenario-dependent random effect $r_T^{scen,i,j}$ to quantify the remaining scenario-dependency of the global HS. That random effect should ideally be small, if the predictors explain precipitation changes sufficiently well. The models excluding and including $r_T^{scen,i,j}$, are subsequently called "standard" and "extended", respectively. All scaling coefficients k_X and standard deviations σ_X^{mod} (and σ_T^{scen}) of the random effects are estimated by a restricted maximum likelihood approach using the R-package "nlme" [*Pinheiro and Bates*, 2000]. To assist comparison of the resulting coefficients, we normalized ΔR_{GHG} and E_{BC} by the reciprocal of the averages across all AOGCMs in 1999.

[13] Besides σ_T^{scen} the Bayesian information criterion (BIC) is used to describe the performance of the statistical model.

4. Performance of the Basic Model Including T, GHG and BC

[14] Figure 1 shows that for some AOGCMs the relation between global-mean precipitation and temperature clearly depends on the considered emission scenario. There is a pronounced difference between the idealized CO_2 doubling and quadrupling runs and the multi-forcing runs, especially for models including BC effects. For some of the BC runs

[1] Auxiliary materials are available in the HTML. doi:10.1029/2010GL045953.

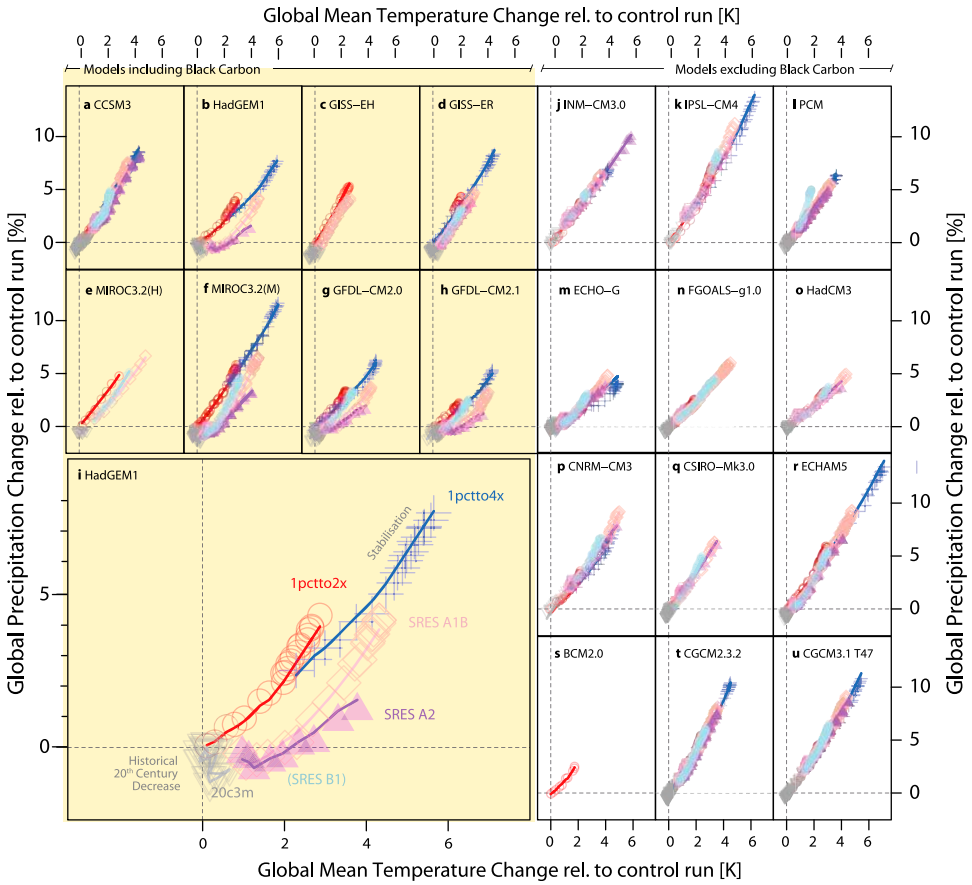

Figure 1. Ten-year averages of relative change in global-mean precipitation with respect to the pre-industrial control run (except of the idealized runs of CCSM3, ECHO-G, CGCM2.3.2, and PCM that branch off the present-day control run) plotted against global-mean temperature change. Color coding indicates different scenarios (red = 1pctto2x, blue = 1pctto4x, grey = 20c3m, violet = commit, pink = sresa1b, purple = sresa2, lightblue = sresb1). Eight AOGCMs took BC into account (panels a to i highlighted in yellow). Projections (best linear unbiased estimates) of our "standard" model based on the three "basic" predictors T, ΔR_{GHG}, and E_{BC} are shown as solid lines. The HadGEM1 diagnosis (panel b) is enlarged for illustrative purposes (panel i).

the forcing effect even leads to a reduction in precipitation in the 20c3m run, an effect also found in some of the BC experiments by *Ming et al.* [2010]. During stabilization, the solely temperature driven increase in precipitation is particularly strong while near-instantaneous radiative effects dampen the increase during other periods [*Wu et al.*, 2010].

[15] Our "standard" model including the "basic" predictors provides a very good fit to the AOGCM data. Global HS is estimated to be 2.2%/K, with σ_T^{mod} = 0.52%/K (see Table 1). This value is smaller than the multimodel mean of 2.76%/K found by *Andrews et al.* [2009] for instantaneous CO_2 doubling experiments performed by slab ocean models but close to the multimodel mean value of 2.4%/K found for the stabilization periods of the idealized model runs performed by a subset of the AR4-AOGCMs also considered here [*Andrews and Forster*, 2010]. The remaining difference might be due to shortcomings of the fixed weightings applied to the adjusted TOA GHG forcings (see section 5) or a slightly different set of AOGCMs. In addition, a part of the temperature dependent response might be attributed to ΔR_{GHG} due to its correlation with ΔT. Increasing GHG forcing and BC emissions leads to a strong near-instantaneous change in precipitation of $-0.42 \pm 0.23\%/(W/m^2)$ for ΔR_{GHG} and $-0.07 \pm 0.02\%/(Mt/yr)$ for E_{BC}. The central value of the scaling coefficients is close to or larger than $2\sigma_X^{mod}$ for all three predictors indicating that the effects are basically consistent across the range of considered AOGCMs (see Table 1).

[16] The inter-scenario variability estimated by the "extended" model versions can be reduced by 50% (from 0.38%/K to 0.19%/K) by including ΔR_{GHG} and E_{BC}. The central estimates are not strongly affected by the inclusion of the scenario dependent random effect r_T^{scen}. Comparing the different models by the BIC clearly shows that the model containing the three "basic" predictors is superior to the reduced one only including ΔT (see Table S1).

5. Sensitivity Analysis

[17] One shortcoming using ΔR_{GHG} are the fixed weightings to calculate the aggregate ΔR_{GHG} from individual adjusted TOA forcings (see auxiliary material). Ideally, each TOA forcing component would be included separately into the regression allowing for AOGCM-specific scaling coefficients for each forcing agent individually. The high correlation of the adjusted TOA forcing time series does however not allow that approach. But, as we include the idealized runs, in which only CO_2 is varied, we can at

Table 1. Central Estimates of the Scaling Coefficients (k_X), Their Standard Errors and the Standard Deviation of the Associated Inter-model Deviations From the Fixed Effects r_X^{mod} [a]

Predictor X	Central Scaling Coefficients k_X	Results for Normalized Predictors		
		k_X	Std. Error	σ^{model}
Standard Model Excluding Inter-scenario Variability of the Scaling Coefficients				
ΔT_{global}	2.191%/K	2.191	0.116	0.517
ΔR_{GHG}	−0.417%/(W/m^2)	−0.803	0.102	0.449
E_{BC}	−0.068%/(Mt/yr)	−0.928	0.096	0.269
ΔT_{global}	2.284%/K	2.284	0.121	0.538
ΔR_{CO2}	−0.525%/(W/m^2)	−1.010	0.160	0.708
$\Delta R_{GHG\backslash CO2}$	−0.150%/(W/m^2)	−0.288	0.216	0.915
E_{BC}	−0.087%/(Mt/yr)	−1.188	0.160	0.440
ΔT_{global}	2.180%/K	2.180	0.127	0.564
ΔR_{GHG}	−0.450%/(W/m^2)	−0.866	0.143	0.630
E_{BC}	−0.068%/(Mt/yr)	−0.925	0.293	0.777
E_{SOx}	−0.001%/(MtS/yr)	−0.047	0.144	0.600
$I_{BC,SOx}$	0.000%/((Mt*MtS)/yr^2)	−0.245	0.114	0.257
F_{volc}	−0.137%/(W/m^2)	−0.133	0.120	0.323
$I_{BC,volc}$	0.043%/(Mt/yr*W/m^2)	0.567	0.164	0.290
F_{solar}	3.094%/(W/m^2)	0.419	0.180	0.677
$I_{BC,solar}$	0.019%/(W/m^2)	0.035	0.263	0.620
Extended Model Allowing for Inter-scenario Variabilities of k_T				
ΔT_{global}	2.365%/K	2.365	0.119	0.523
ΔR_{GHG}	−0.510%/(W/m^2)	−0.981	0.127	0.564
E_{BC}	−0.068%/(Mt/yr)	−0.924	0.060	0.150
ΔT_{global}	2.346%/K	2.346	0.102	0.444
ΔR_{CO2}	−0.503%/(W/m^2)	−0.967	0.130	0.571
$\Delta R_{GHG\backslash CO2}$	−0.359%/(W/m^2)	−0.691	0.226	0.940
E_{BC}	−0.081%/(Mt/yr)	−1.100	0.104	0.254

[a]Estimates are based on the "standard" model only including inter-model random effects and the "extended" model additionally allowing for inter-scenario deviation from k_T. Central estimates provided in the first column refer to variables given in standard units while the results given in the other columns refer to variables (except of temperature) that are normalized towards 1999 or 1991 in the case of volcanic forcing, respectively.

least split up ΔR_{GHG} into the tropospheric forcing induced by CO_2(ΔR_{CO2}), and the remainder ($\Delta R_{GHG\backslash CO2}$). Including both components into the statistical model provides larger coefficients for the CO_2 component and smaller ones for $\Delta R_{GHG\backslash CO2}$ (see Table 1). This indicates that our weights for aggregating ΔR_{GHG} might have to be reduced for the other GHGs in comparison to CO_2. The estimated global HS of 2.3%/K is slightly closer to the estimate of *Andrews and Forster* [2010].

[18] We also tested an array of additional predictors. These are sulfate emissions (E_{SOx}), volcanic forcing (F_{volc}), solar forcing (F_{solar}), interaction effects between BC and sulfate aerosols (i.e., the product of (normalized) BC and sulfate emissions, $I_{BC,SOx}$), and analogously $I_{BC,volc}$ and $I_{BC,solar}$. While E_{SOx} and F_{solar} were normalized analogously to E_{BC} and ΔR_{GHG}, F_{volc} was normalized with respect to 1991, the year of the Pinatubo eruption. Stepwise inclusion of these predictors still reduces the BIC but in smaller steps (see Table S1). The "standard" model including additional predictors improves only slightly on the model with the "basic" predictors (see Figure S6). There is nearly no further reduction in σ_T^{scen} estimated by the "extended" model.

[19] While the scaling coefficients of the basic predictors are relatively stable across the different model versions, the effects of the additional components turn out to be smaller and less consistent across AOGCMs as evident from the comparison of the central estimates and their inter-AOGCM variations σ_X^{model} (see Table 1). The effect of E_{SOx} per unit mass of emissions is more than one order of magnitude smaller than the BC effect and not significantly different from zero. That is expected from TOA and surface forcings being nearly identical for sulfate aerosols. However, there seems to be a larger interaction effect indicating that precipitation is reduced when SOx emissions are increased in presence of BC. This might be due to more absorption of shortwave radiation by BC when shortwave radiation is scattered by sulfate aerosols – an interaction effect that depends on the vertical distribution of both BC and sulfates. The sign of the scaling coefficient related to F_{volc} is consistent with the expectation that a reduction in shortwave radiation passing the troposphere leads to less absorption of shortwave radiation. The absolute value of the scaling coefficients is relatively small as expected from the fact that TOA and surface forcing of volcanic aerosols do not differ strongly.

[20] The signs of the other scaling coefficients found for $I_{BC,volc}$, F_{solar}, and $I_{BC,solar}$ are not consistent with our expectation based on tropospheric energy budget considerations. Increases in stratospheric aerosols should reduce the amount of shortwave radiation reaching the troposphere, which in turn should lead to less absorption of shortwave radiation by BC particles and increased precipitation. Similarly, increasing solar forcing should lead to (slightly) more shortwave absorption in the troposphere and small decreases in precipitation as also seen in the experiments by *Andrews et al.* [2010]. In both cases, we find however a positive scaling coefficient with the reasons for this disagreement being presently unclear. The common feature of these "problematic" forcings is that their variations are limited to the 20c3m run which represents a relatively small part of the whole data set. Analysing the 20c3m runs *Lambert and Allen* [2009] also found positive scaling coefficients for their forcing component that combines volcanic and tropospheric sulfate aerosol forcings. There might be correlated forcings that influence these scaling coefficients. As well, the regression could erroneously relate a part of the temperature dependent response to these forcing components.

[21] We trained our statistical model on all available CMIP3 scenarios. Thus, the question is how suitable our approach might be for projecting changes for non-calibrated scenarios. We tested the prediction skill of the "standard" model with our "basic" predictors by excluding one scenario after another from the regression and by predicting changes in relative precipitation for the excluded scenario. As illustrative goodness of fit measure, we computed a root mean square error (RMSE) of 0.38% precipitation changes across all scenarios. This can be compared to a RMSE of 0.28% when all available data points are used for calibration. Given the overall magnitude of modeled precipitation changes of up to 5% and 10%, the prediction skill of our statistical approach is comparatively good (see Figure S7).

6. Conclusions

[22] Our study contributes to the theoretical understanding of modeled global-mean precipitation changes. Going beyond a simple linear scaling with global-mean tempera-

tures, we have shown that modeled global HS and its variations across scenarios are remarkably well reproduced by three predictors: global-mean temperature change, tropospheric GHG forcing and BC emissions. We presented here the first study analyzing a comprehensive set of AOGCMs across the full range of future SRES and idealized scenarios from the CMIP3 archive. We were able to quantify the distinct precipitation sensitivities by drawing information from the time-varying changes within and the comparison of changes across different scenarios. Our analysis is based on the assumption that the tropospheric GHG and BC forcing is proportional to the TOA GHG forcing and BC emissions, respectively. This assumption needs further validation by future modeling studies.

[23] Given the skill for predicting global-mean precipitation changes, multiple scenarios could now be modeled including those not yet run by a comprehensive set of AOGCMs. The forthcoming datasets of CMIP5, for which AOGCMs are likely driven with a more standardized and comprehensive set of forcings for more model years, will allow a verification and refinement of this statistical approach to project and explain global-mean precipitation changes across a wide range of future scenarios. Particularly, the RCP3PD scenario including periods of decreasing forcing and the abrupt CO_2 quadrupling experiments (K. E. Taylor et al., A summary of the CMIP5 experiment, 2009, http://cmip-pcmdi.llnl.gov/cmip5/docs/Taylor_CMIP5_design.pdf) might add valuable information to decouple the slow temperature related and the fast GHG forcing related responses.

[24] **Acknowledgments.** KF and MM were supported by the UFO-PLAN project (FKZ 370841103) by the German Federal Environment Agency. We acknowledge the modeling groups, the Program for Climate Model Diagnosis and Intercomparison (PCMDI) and the WCRP's Working Group on Coupled Modelling (WGCM) for making available the WCRP CMIP3 multi-model dataset. Support of this dataset is provided by the Office of Science, U.S. Department of Energy. In particular we thank Vaishali Naik and Larry Horowitz for providing BC emission data for the GFDL model runs and Tim Johns for providing information about the BC data used for the HadGEM1 runs. We acknowledge Toru Nozawa providing the BC data for the MIROC model runs. Gary Strand provided the BC-scaling coefficients used within the CCSM3 runs and Dorothy Koch provided the information about the GISS BC input.

References

Allen, M. R., and W. J. Ingram (2002), Constraints on future changes in climate and the hydrological cycle, *Nature*, *419*, 224–232, doi:10.1038/nature01092.

Andrews, T., and P. M. Forster (2010), The transient response of global-mean precipitation to increasing carbon dioxide levels, *Environ. Res. Lett.*, *5*, 025212, doi:10.1088/1748-9326/5/2/025212.

Andrews, T., P. M. Forster, and J. M. Gregory (2009), A surface energy perspective on climate change, *J. Clim.*, *22*, 2557–2570, doi:10.1175/2008JCLI2759.1.

Andrews, T., P. M. Forster, O. Boucher, N. Bellouin, and A. Jones (2010), Precipitation, radiative forcing and global temperature change, *Geophys. Res. Lett.*, *37*, L14701, doi:10.1029/2010GL043991.

Arkin, P. A., T. M. Smith, M. R. P. Sapiano, and J. Janowiak (2010), The observed sensitivity of the global hydrological cycle to changes in surface temperature, *Environ. Res. Lett.*, *5*, 035201, doi:10.1088/1748-9326/5/3/035201.

Dong, B., J. M. Gregory, and R. T. Sutton (2009), Understanding land-sea warming contrast in response to increasing greenhouse gases. Part I: Transient adjustment, *J. Clim.*, *22*, 3079–3097, doi:10.1175/2009JCLI2652.1.

Held, I. M., and B. J. Soden (2006), Robust responses of the hydrological cycle to global warming, *J. Clim.*, *19*, 5686–5699, doi:10.1175/JCLI3990.1.

Lambert, F. H., and M. R. Allen (2009), Are changes in global precipitation constrained by the tropospheric energy budget?, *J. Clim.*, *22*, doi:10.1175/2008JCLI2135.1.

Lambert, F. H., and N. E. Faull (2007), Tropospheric adjustment: The response of two general circulation models to a change in insolation, *Geophys. Res. Lett.*, *34*, L03701, doi:10.1029/2006GL028124.

Lambert, F. H., and M. J. Webb (2008), Dependency of global mean precipitation on surface temperature, *Geophys. Res. Lett.*, *35*, L16706, doi:10.1029/2008GL034838.

Liepert, B. G., and M. Previdi (2009), Do models and observations disagree on the rainfall response to global warming?, *J. Clim.*, *22*, 3156–3166, doi:10.1175/2008JCLI2472.1.

Meinshausen, M., S. C. B. Raper, and T. M. L. Wigley (2008), Emulating IPCC AR4 atmosphere-ocean and carbon cycle models for projecting global-mean, hemispheric and land/ocean temperatures: MAGICC 6.0, *Atmos. Chem. Phys. Discuss.*, *8*, 6153–6272, doi:10.5194/acpd-8-6153-2008.

Ming, Y., V. Ramaswamy, and G. Persad (2010), Two opposing effects of absorbing aerosols on global-mean precipitation, *Geophys. Res. Lett.*, *37*, L13701, doi:10.1029/2010GL042895.

Mitchell, J. F. B., C. A. Wilson, and W. M. Cunnington (1987), On CO_2 climate sensitivity and model dependence of results, *Q. J. R. Meteorol. Soc.*, *113*, 293–322, doi:10.1256/smsqj.47516.

Pinheiro, J. C., and D. M. Bates (2000), *Mixed-Effects Models in S and S-PLUS, Stat. Comput.*, Springer, New York.

Previdi, M. (2010), Radiative feedbacks on global precipitation, *Environ. Res. Lett.*, *5*, 025211, doi:10.1088/1748-9326/5/2/025211.

Ramanathan, V., P. J. Crutzen, J. T. Kiehl, and D. Rosenfeld (2001), Aerosols, climate, and the hydrological cycle, *Science*, *294*, 2119–2124, doi:10.1126/science.1064034.

Trenberth, K. E., et al. (2007), Observations: Surface and atmospheric climate change, in *Climate Change 2007: The Physical Science Basis. Contribution of Working Group I to the Fourth Assessment Report of the Intergovernmental Panel on Climate Change*, edited by S. Solomon et al., pp. 235–336, Cambridge Univ. Press, Cambridge, U. K.

Wentz, F. J., L. Ricciardulli, K. Hilburn, and C. Mears (2007), How much more rain will global warming bring?, *Nature*, *317*, 233–235.

Wu, P., R. Wood, J. Ridley, and J. Lowe (2010), Temporary acceleration of the hydrological cycle in response to a CO_2 rampdown, *Geophys. Res. Lett.*, *37*, L12705, doi:10.1029/2010GL043730.

Yang, F., A. Kumar, M. E. Schlesinger, and W. Wang (2003), Intensity of hydrological cycles in warmer climates, *J. Clim.*, *16*, 2419–2423, doi:10.1175/2779.1.

T. Andrews and P. Forster, School of Earth and Environment, University of Leeds, Leeds LS2 9JT, UK.

K. Frieler, M. Meinshausen, and T. Schneider von Deimling, Earth System Analysis, Potsdam Institute for Climate Impact Research, Telegrafenberg A26, D-14412 Potsdam, Germany. (katja.frieler@pik-potsdam.de)